ELSEVIER

Earth and Planetary Science Letters 200 (2002) 387–400

EPSL

www.elsevier.com/locate/epsl

The loess record in southern Tajikistan and correlation with Chinese loess

Z.L. Ding [a,*], V. Ranov [b], S.L. Yang [a], A. Finaev [c], J.M. Han [a], G.A. Wang [a]

[a] *Institute of Geology and Geophysics, CAS, Beijing 100029, PR China*
[b] *Institute of History, Archaeology and Ethnography, Tajikistan Academy of Science, 734025 Dushanbe, Tajikistan*
[c] *Institute of Geology, Tajikistan Academy of Sciences, 734025 Dushanbe, Tajikistan*

Received 11 January 2002; received in revised form 28 March 2002; accepted 30 March 2002

Abstract

In the present study, the Chashmanigar loess–soil sequence in southern Tajikistan is studied; this loess section has a paleomagnetic basal age of about 1.77 Myr. Magnetic susceptibility, color reflectance and grain size were systematically measured for closely spaced samples from the section. Paleosols consistently have a finer grain size distribution, higher magnetic susceptibility, redder color reflectance and lower dust sedimentation rate than loess horizons, suggesting a colder, drier and dustier environment during glacial periods than in interglacial periods. The grain size record was tuned to variations in obliquity and precession of the Earth's orbit. The resulting magnetic susceptibility, grain size and color reflectance time series all show well-expressed astronomical periodicities during the Pleistocene. The mid-Pleistocene climate transition, characterized by a shift of dominant climatic periods from 41 kyr to 100 kyr at about 1.0–0.8 Myr, is clearly documented in these proxy records. Comparison of the Chashmanigar loess record with the Lingtai loess section in China and the ODP site 677 $\delta^{18}O$ record shows that during the entire Pleistocene, the climate cycles recorded by the Central Asian loess can be well correlated to the Chinese loess and deep-sea oxygen isotope records. It is suggested that alternations of loess and soil horizons both in Central Asia and China could be basically forced by global ice volume variations, although different wind systems have controlled the Pleistocene loess transport and sedimentation in the two areas.

Keywords: Central Asia; loess; eccentricity; orbital forcing; climate change; Pleistocene; paleoclimatology

1. Introduction

Continental loess deposits have long been regarded as one of the most important archives of Pleistocene climatic evolution [1–7]. On the globe, the thickest and most complete loess records are preserved in the Chinese Loess Plateau and Central Asia [5,8–12]. The formation of the loess–paleosol sequence in the Chinese Loess Plateau is closely associated with variations in the East Asian monsoon system [9,13,14], whereas the regional westerly winds controlled the transport and sedimentation of the loess in Central Asia. Therefore, correlation of loess records between the two far-separated regions would be invaluable in the understanding of the forcing mechanisms for long-term hemispheric or global climate evolution

* Corresponding author. Fax: +86-10-62-01-08-46.
E-mail address: zlding@95777.com (Z.L. Ding).

0012-821X/02/$ – see front matter
PII: S0012-821X(02)00637-4

[11]. In recent years, abundant information on regional climatic changes of the Pleistocene has been derived from the Chinese loess sequences, based on the analyses of various climate proxies. Comparatively, studies of climatic changes registered in the Central Asian loess have received less attention except for a magnetic susceptibility record of the past 0.8 Myr provided by Shackleton and co-authors [11]. This thus hinders the detailed comparison between long-term climatic evolution of the two loess regions.

Recently, we conducted magnetic susceptibility, grain size and color reflectance analyses of the Chashmanigar loess section in southern Tajikistan, which spans the past 1.77 Myr. The Chashmanigar loess record on an orbital time scale was then correlated with the Lingtai loess record of the Chinese Loess Plateau, the eolian mass accumulation rate records of the Northwest Pacific and an oxygen isotopic record of deep-sea sediments. This paper presents the results of the studies, and briefly addresses the paleoclimatic implications of the Tajik loess record.

2. Setting and general nature

The Chashmanigar loess section (latitude 38°23′32″N, longitude 69°49′57″E) is situated in southern Tajikistan where loess deposits are widely distributed on river terraces and piedmonts. Although the so-called 'Loess Yuan' – the broad, flat, high tablelands in the Chinese Loess Plateau – is not seen in southern Tajikistan, loess hills there can reach up to 200 m in height. Stratigraphic and chronological studies have previously shown that the Central Asian loess began to accumulate about 2–2.5 Myr ago, and the loess–soil sequences at different sites can be correlated with each other [8,15,16].

Loess accumulation in southern Tajikistan is tightly related to the geographic and atmospheric conditions in the area. The great deserts such as Karakum and Kyzylkum are situated directly to the west and northwest of the loess region, and the lofty Pamir Plateau with an average elevation of more than 3000 m to the east (Fig. 1b). The vast deserts, with sparse vegetation cover, can provide an enormous quantity of eolian dust for the loess region. Modern atmospheric observations [16,17] show that the frequency of dust storms in the deserts is over 50 days per year. The climate in this loess region is characterized by hot, dry summers and mild, wet winters. During the dry summer season, dust storms prevail in the deserts, and the deflated eolian dust is carried by westerly air streams to the east, where it rapidly settles down when the air currents meet the Pamir Plateau. During the wet winter season, dust storms basically disappear in the deserts with the increase of precipitation. Therefore, the occurrence and transport of atmospheric dust in Central Asia significantly differ from that in the Chinese Loess Plateau, where dust storms occur in the dry, cold winter season and are transported by the northwesterly winter monsoon winds.

At present, the mean annual temperature and precipitation at Chashmanigar are about 11°C and 842 mm, respectively. The Chashmanigar loess section, with a thickness of about 205 m, is underlain by gravel sediments. The loess sequence is composed of many loess and paleosol horizons. The loess horizons show a yellowish color and a massive structure, while the paleosols are characterized by a brownish or reddish color, a subangular blocky structure and more or less translocated clay coatings. In general, there is a carbonate nodule horizon directly below the paleosols. The stratigraphic structure of the section can be roughly subdivided into two parts. The paleosols in the lower part of the section are relatively thin and closely spaced, whereas they are much thicker and separated by thick loess layers in the upper part. These features are almost the same as those found in the Chinese Loess Plateau. However, although the loess–paleosol sequence at Chashmanigar can be generally correlated in the field with the Chinese loess, some outstanding stratigraphic markers such as L9 and L15 in the Loess Plateau [2] are indistinct in the Chashmanigar section.

A total of 29 paleosols are distinguishable above a depth of 195 m at Chashmanigar. The lowermost part of the section is unfortunately covered by slumps. In the field, we correlated the loess–soil sequence at Chashmanigar with

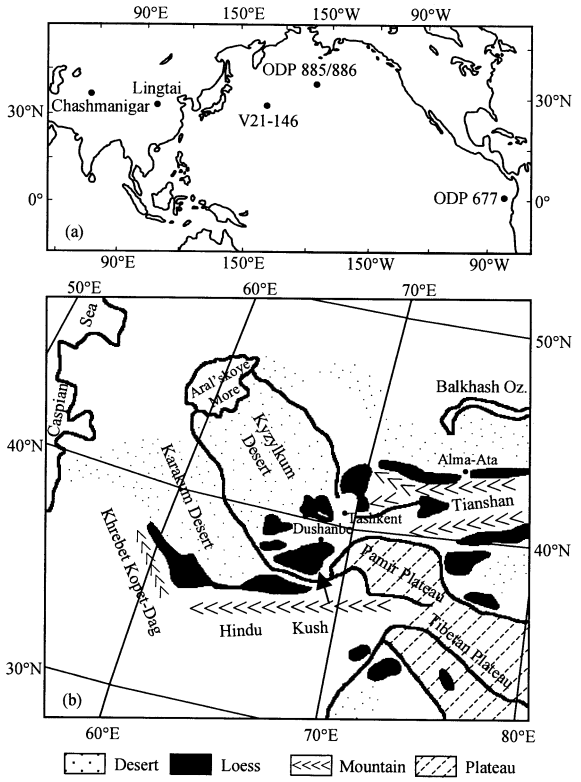

Fig. 1. Schematic maps (a) showing the localities where the records mentioned in the paper are obtained, and (b) showing the distribution of loess, deserts, and mountains in Central Asia (adopted from [2]). The locality of the Chashmanigar loess section is indicated by the solid arrow.

the S0–S24 portion of the Chinese loess. Samples were taken at 5 cm intervals from the top to a depth of 161.8 m, and at 10 cm intervals for the lowermost part of the section. A total of 3542 samples were collected. In addition, paleomagnetic samples were taken from the positions where previous work indicated that paleomagnetic events occur [8]. The paleomagnetic samples are concentrated on the B/M boundary, the Jaramillo subchron and the lowermost part of the section.

3. Stratigraphy and climatic records

Magnetic susceptibility, color reflectance and grain size were measured for all the samples collected at Chashmanigar, using a Bartington MS2 susceptibility meter, a Minolta-CM2002 spectrophotometer and a SALD-3001 laser diffraction particle analyzer, respectively. The grain size analysis procedures are described in [18]. The paleomagnetic samples were analyzed with a 2G three-axis Cryogenic Magnetometer in the Institute of Geology and Geophysics, CAS.

Down-section changes in median grain size, magnetic susceptibility, and chromaticity (a^*) at Chashmanigar are shown in Fig. 2, together with the paleomagnetic results. The numbering of the loess–soil units for the entire Chashmanigar section is adopted from the Chinese loess [5], while the traditional soil designation [8] for the upper part of the section is retained. Loess particle changes are believed to be mainly related with changes in both the intensity of the transporting wind system and the distance of the depositional area to the source region [9,19,20]. In the Chashmanigar section, median grain size in loess horizons is consistently coarser than in paleosols, suggesting that during glacial periods, the intensity of the regional westerly winds was significantly enhanced and/or the deserts in Central Asia were expanded, with respect to interglacial periods. There is a clear upward increase in particle sizes of loess horizons from the bottom of the section up to L6 (Fig. 2). Except for the wide variation in particle sizes between loess and paleosol units, a second-order grain size change is also found within some loess or paleosol horizons such as S1, L2 and L6 (Fig. 2).

In the Chinese loess, magnetic susceptibility records are widely used as a proxy for changes in summer monsoon precipitation [13,21,22]. Susceptibility values are consistently higher in paleosols than in the underlying loess beds at Chashmanigar (Fig. 2), implying that pedogenic origin of magnetic minerals may also be an important process during the development of the paleosols in the Central Asian loess. However, the paleoclimatic interpretation of the magnetic susceptibility variability at Chashmanigar is complicated by the fact that there is an upward increase of loess susceptibility. From the bottom to the top of the section, susceptibility values of the loess beds gradually increase from about 10 to 50×10^{-8} $m^3\cdot kg^{-1}$ (Fig. 2). This increase in loess suscepti-

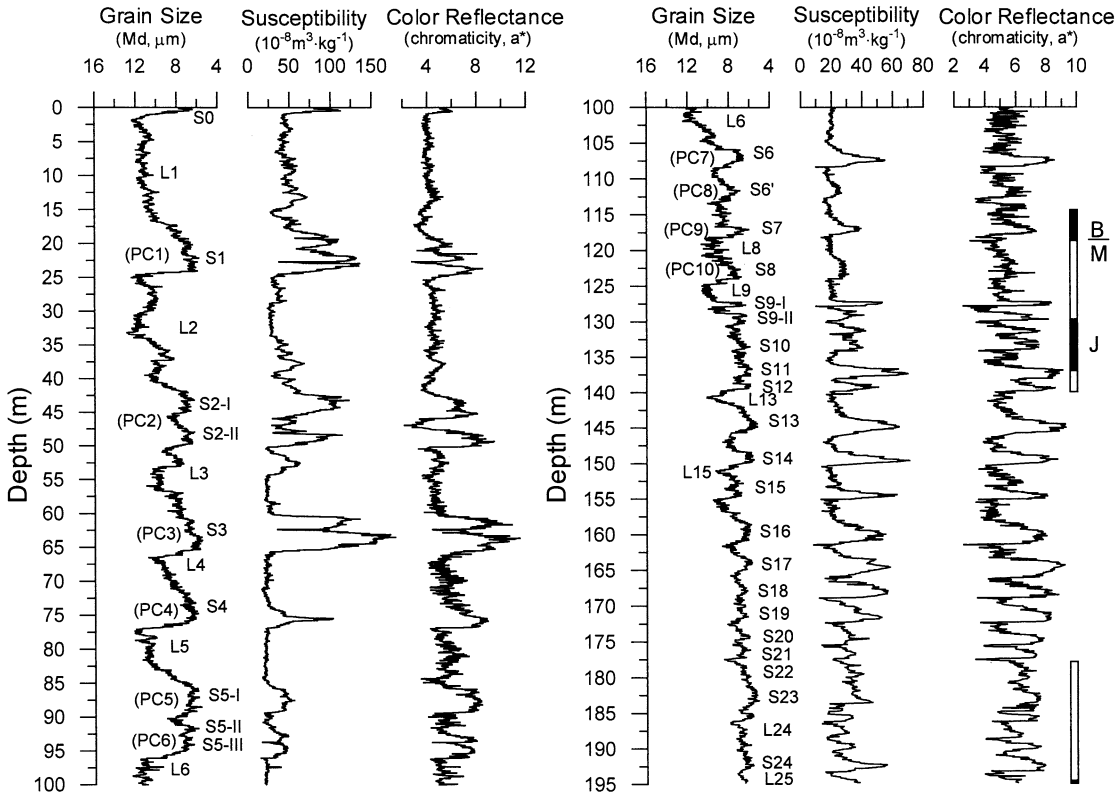

Fig. 2. Median grain size, magnetic susceptibility, and color reflectance records of the Chashmanigar loess section, together with paleomagnetic analytical results. The loess–soil units are labeled with both the Li–Si system as used in the Chinese loess and the PCi system traditionally used in Tajikistan. The axes for the grain size curves are reversed.

bility values may not be caused exclusively by pedogenic enhancement, since such a pedogenic increase trend was not recognized in the field for the loess horizons. Susceptibility values are mostly below 60×10^{-8} $m^3{\cdot}kg^{-1}$ for the paleosols below S4, whereas the three paleosol complexes above S4 have susceptibility values higher than 100×10^{-8} $m^3{\cdot}kg^{-1}$ (Fig. 2).

A Minolta-CM2002 spectrophotometer can give the $L^*a^*b^*$ color space of the samples being measured. In this color space, L^* indicates lightness and a^* and b^* are the chromaticity coordinates. In the a^*, b^* chromaticity diagram, the a^* and b^* indicate color directions: $+a^*$ is the red direction, $-a^*$ is the green direction, $+b^*$ is the yellow direction, and $-b^*$ is the blue direction. In the Chashmanigar loess–paleosol sequence, L^* values are higher in loess horizons than in paleosols (not shown), being consistent with the observation that loess beds are generally lighter than paleosols. In the field, the most visible color difference between loess and paleosol horizons is that paleosols are much redder than loess beds. Actually, color is a most important criterion in field work for distinguishing paleosols from loess deposits. The chromaticity a^* values in paleosols are about two times as high as in loess beds at Chashmanigar, coinciding with field observations. Variation in a^* values is more consistent than the grain size and susceptibility records; they are mostly around 4 in loess beds, and around 8 in paleosols. The highest a^* values (about 10) in the entire sequence occur in S3.

According to paleomagnetic measurements, the Brunhes/Matuyama magnetic reversal occurred in loess unit L8 or between PC9 and PC10, and the

upper and lower boundaries of the Jaramillo subchron are defined, respectively, within L10 (between S9 and S10) and at the bottom of S11 (Fig. 2). These results are in agreement with previous work [8] and the Chinese loess magnetostratigraphy [4,23]. One previous study [8] found that the Olduvai subchron occurs in the lowermost part of the Chashmanigar section. In the present study, this part was not sampled because of poor exposure. However, magnetic remanence data were measured for the stratum from S22 to L25. All the samples show reversed polarity except for the lowermost sample (Fig. 2). In the Chinese loess sequence, the upper boundary of the Olduvai is found in the middle of loess unit L25 [5,24]. As the Chashmanigar loess–soil sequence is well correlated with the Chinese loess, we infer that the Chashmanigar section has been sampled in the present study down to the upper boundary of the Olduvai, thus suggesting a basal age of about 1.77 Myr for the Chashmanigar loess.

4. Orbital time scale

It has long been demonstrated that the cyclic change of the Quaternary climate was initially forced by variations in the Earth's orbital geometry [25–27]. The theoretically calculated astronomical records can thus be used to fine-tune time scales of climatic proxy records. This approach has achieved great success in developing climatic time scales of deep-sea and loess sediments for the entire Quaternary period [9,28–31]. As shown in Fig. 2, the major loess–soil units recognized in the Chinese loess are also recorded by the Chashmanigar loess section, thus suggesting that near-continuous dust deposition at Chashmanigar has been preserved and the precondition for establishing an orbital time scale is satisfiable for the section.

Shackleton et al. [11] have tuned the magnetic susceptibility record above S8 (PC10) of the Karamaidan loess section in Tajikistan to orbital changes. Here we tune the whole Chashmanigar grain size curve simultaneously to the calculated changes in obliquity and precession of the Earth's orbit [32], with the following procedures. Firstly, the phase relations between the grain size cycles and the corresponding obliquity and precession cycles must be assumed because loess chronological studies cannot provide accurate constraints on the relations. Since previous loess studies [11,14] have shown that climate variability in both southern Tajikistan and the Chinese Loess Plateau has been forced initially by changes in global glacial-boundary conditions, we assumed an in-phase change of the loess record relative to $\delta^{18}O$ records. In the tuning targets, therefore, the obliquity curve is lagged to 8 kyr and the precessional index curve to 5 kyr, both values being derived from [27]. As will be seen below, these lags remain relatively stable for the whole tuned climate record.

Secondly, we established an initial time scale for the Chashmanigar grain size record, using the magnetic reversals (Fig. 2) as time controls. In doing so, the orbital time scale of the Karamaidan loess section [11] is used for the upper part (above S8). For the lower part, we assign each of the grain size peaks within thick loess horizons to a precession cycle, and each of the paleosols to an obliquity cycle except for S13 and S23. S13 and S23 are both exceptionally thick soils. Each of them is interpreted to correspond to three precession cycles. The S13 paleosol complex is correlative to marine oxygen isotope stage 35 [31], which consists of three precession-related cycles. For S23, an additional precession-related cycle at the transition between its lowermost part to the uppermost of L24 is recognizable from the climate proxy records shown in Fig. 2. It should be indicated that in establishing the initial time scale, the lock-in depth of paleomagnetic reversals [33] is considered. As the lock-in effect always makes the measured paleomagnetic reversals downward in loess sequences, they have to be displaced upward relative to the proxy curves. To assign the paleosol directly above each of the reversals to a height of obliquity that should be slightly younger than the age of the measured paleomagnetic boundary, the upper and lower boundaries of the Jaramillo Chron have been displaced upwards by several tens of centimeters, and the B/M boundary by over 1 m (see Fig. 3).

Thirdly, we repeatedly used two phase-free dig-

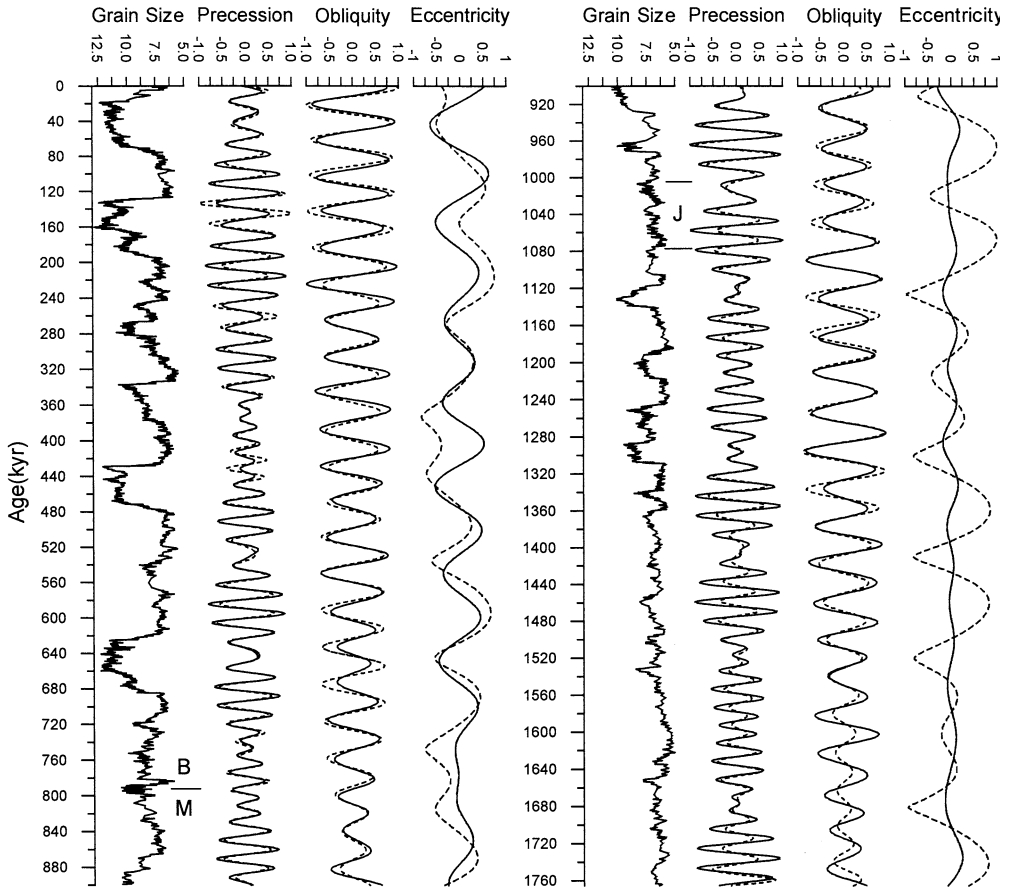

Fig. 3. Grain size time series of the Chashmanigar loess section, and filtered precession, obliquity and eccentricity signals (dashed lines) versus lagged theoretical orbital precession (reversed) and obliquity and non-lagged eccentricity records (solid lines). The filtered precession, obliquity and eccentricity signals from the grain size time series have a Central period of 22, 41 and 100 kyr, respectively. The theoretical orbital data are from Berger and Loutre [32]. The filtered signals and orbital records are all normalized. The positions of the measured B/M paleomagnetic reversal and the upper and lower boundaries of the Jaramillo Chron are shown with respect to the grain size curve.

ital filters respectively with central periods of 41 kyr and 22 kyr to extract these frequency components from the grain size record on the initial time scale, and matched the phase of each cycle of the filtered curves to the phase of the corresponding cycle in the target curves by manually adding new time control points and by assuming uniform deposition rate between these points. The filter length is 50 kyr for the 22 kyr central period and 130 kyr for the 41 kyr period, respectively. This tuning results in an intermediate time scale for the grain size record. Finally, we applied the Dynamic Optimization method to automatically add new time control points to the grain size record on the intermediate time scale. This method iteratively adjusts each of the climatic data in order to achieve the highest correlation coefficients between the orbital frequency curves filtered from the grain size record and the target curves [34].

Fig. 3 shows the final version of the tuned Chashmanigar grain size time scale (here called the CGS time scale) and a comparison of the filtered obliquity, precession and eccentricity components from the grain size record on the CGS time scale with variations in the three orbital elements of the Earth. For both the obliquity and

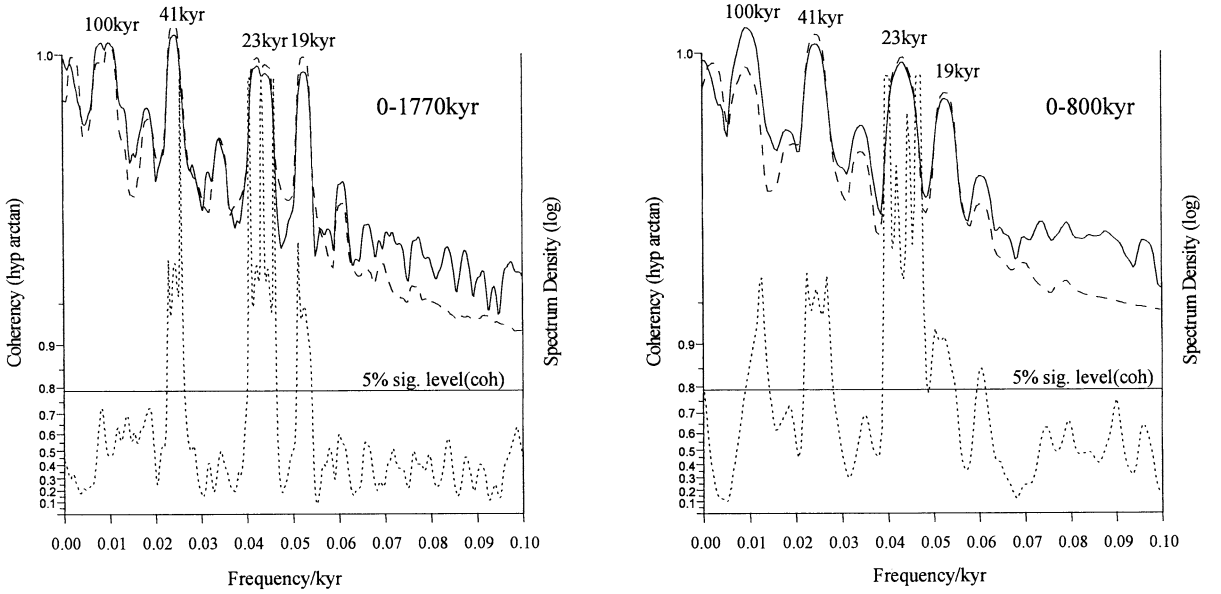

Fig. 4. Coherency and variance spectra calculated from the Chashmanigar grain size and theoretical orbital records over the time intervals 0–1.77 Myr (left) and 0–0.8 Myr (right). Two signals have been processed: (1) ETP, a signal formed by normalizing and adding variations in orbital eccentricity, obliquity, and precession (reversed); (2) the Chashmanigar grain size record on the CGS time scale (Fig. 3). Top: variance spectra (solid line: cross-spectrum between the two signals; dashed line: ETP variance spectrum), plotted on arbitrary log scales. Bottom: coherency spectrum plotted on a hyperbolic arctangent scale and provided with a 5% significance level. Frequencies are in cycles per 1000 yr.

precession signals, almost all the filtered cycles fit the theoretical versions, with the amplitudes being fairly similar to the astronomical forcing except for the lowermost part of the obliquity record. The correlation coefficients between the filtered orbital components and the theoretical orbital curves are 0.915 for obliquity and 0.924 for precession. In addition, the 100 kyr period component filtered from the time series also shows a roughly in-phase change with the orbital eccentricity record over the past 0.8 Myr.

We then used a cross-spectral comparison of the resulting grain size time series with the orbital data to evaluate the CGS time scale. Fig. 4 shows the results of the cross-spectral analysis between the grain size data plotted on the CGS time scale and the theoretical orbital record (ETP curve). The ETP curve was formed by stacking the normalized eccentricity and obliquity curves and the normalized and reversed precession index curve [32]. In the last 1.77 Myr, cross-spectral analysis (Fig. 4, left) shows that the Chashmanigar grain size time series closely matches the orbital signals at the periods of obliquity (41 kyr) and precession (23 and 19 kyr) with coherencies higher than 0.95. These peaks in the coherency spectrum coincide well with the peaks in the ETP spectrum. The coherency at the eccentricity period (100 kyr) is insignificant during the entire Pleistocene (Fig. 4, left). In the last 0.8 Myr, however, we measured a coherency of about 0.96 at the 100 kyr period (Fig. 4, right), this being well above the 5% significance level.

To monitor temporal evolution in the phase relation, we used an evolutive coherency method to do cross-spectral analysis between the CGS time scale and the ETP record. Coherency was calculated with record length of 400 kyr with a 10 kyr offset, and with the degree of freedom being 6. Results show that the assumed time lags, i.e. 8 kyr for obliquity and 5 kyr for precession, remain quite stable for the entire sequence. The averaged time lag is 7.89 kyr at the 41 kyr period and 4.77 kyr at the 19 kyr period, respec-

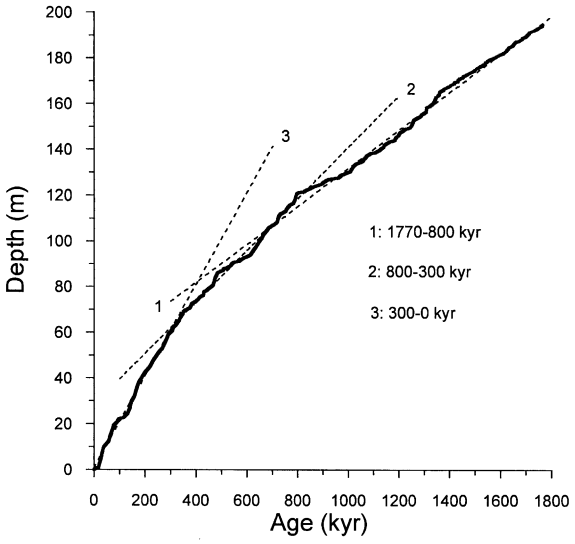

Fig. 5. Age–depth plot of the Chashmanigar loess sequence.

tively. At the 23 kyr period, the averaged time lag is 5.37 kyr before 1.3 Myr and 4.84 kyr after 1.3 Myr. These cross-spectral analyses therefore suggest that this tuned time scale is tightly constrained, thereby providing the opportunity to assess the time duration of each of the loess–soil units at Chashmanigar (Table 1).

The orbital time scale allows calculation of dust deposition rate changes for the Chashmanigar loess section. The depth–age curve (Fig. 5) can be roughly subdivided into three parts. Over the time interval 1.77–0.8 Myr, the averaged dust deposition rate is about 7.1 cm/kyr. It increases to about 13.4 cm/kyr between 0.8 and 0.3 Myr. The highest averaged deposition at Chashmanigar is found in the last 0.3 Myr. It is about 20 cm/kyr, almost three times as high as that in the early Pleistocene. The upward increase in the averaged dust deposition rate in the Chashmanigar loess section implies that the deserts in Central Asia may have experienced a stepwise expansion in the Quaternary, since dust deposition rates can be used as an indicator of aridity in source areas [35].

5. Orbital periodicities and climate correlation

To examine the time-dependent characteristics of climatic frequencies registered in the Chashmanigar loess section, we conducted spectral analyses on the grain size, magnetic susceptibility, and color reflectance records plotted on the orbital time scale (Fig. 6). The three time series all show a clearly time-dependent feature of the climatic periodicities. In the last 1.0 Myr or so, the strongest power is centered at about 100 kyr, with relatively weak powers of the obliquity (41 kyr) and precession (23 and 19 kyr). During the past 0.6 Myr, a power centered at about 30 kyr is also evident in all the three signals. Over the time interval 0.8–1.77 Myr, the 100 kyr eccentricity-associated pe-

Table 1
Age estimates of soil units from the CGS time scale

Unit	Top (Myr)	Bottom (Myr)	Unit	Top (Myr)	Bottom (Myr)
S0	0.000	0.015	S11	1.060	1.071
S1	0.076	0.128	S12	1.105	1.117
S2-1	0.194	0.219	S13	1.141	1.189
S2-2	0.230	0.243	S14	1.217	1.245
S3	0.307	0.333	S15	1.256	1.286
S4	0.382	0.426	S16	1.309	1.335
S5	0.507	0.619	S17	1.346	1.359
S6	0.685	0.712	S18	1.373	1.403
S6′	0.725	0.736	S19	1.437	1.451
S7	0.782	0.788	S20	1.482	1.495
S8	0.798	0.867	S21	1.507	1.519
S9-1	0.930	0.954	S22	1.540	1.571
S9-2	0.972	1.009	S23	1.596	1.623
S10	1.020	1.031	S24	1.713	1.738

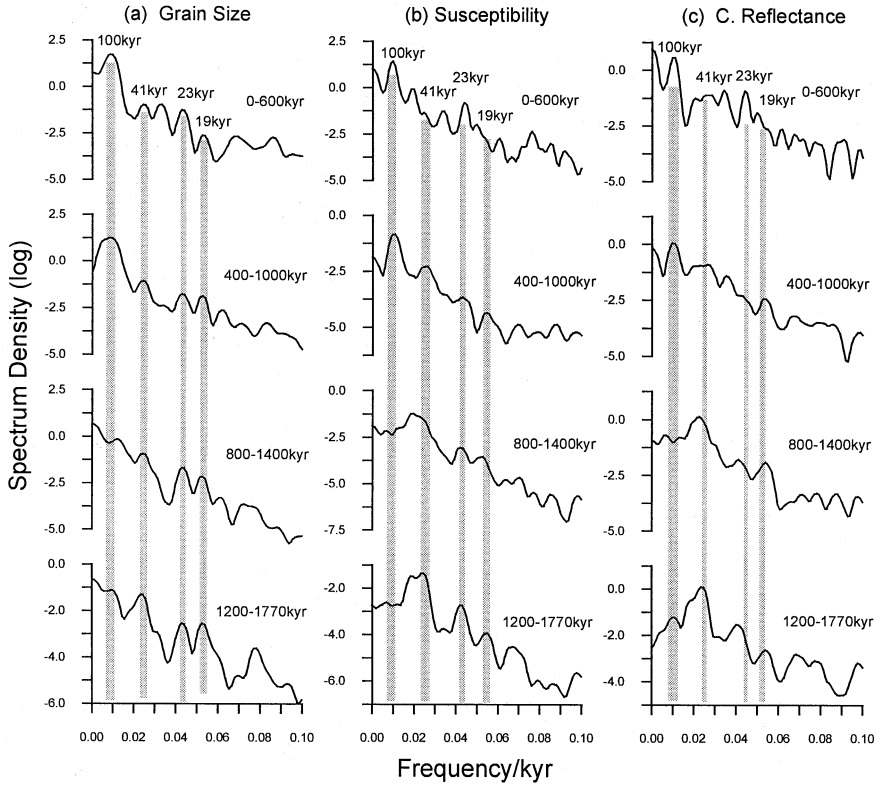

Fig. 6. Spectra of the Chashmanigar grain size, magnetic susceptibility, and color reflectance records derived from CGS orbital time scale over four different time intervals. Frequencies are in cycles per 1000 yr.

riodicity is not detected, whereas the 41 kyr obliquity power becomes dominant. Therefore, these spectral analyses suggest that there is a clear shift of dominant periodicities at about 0.8–1.0 Myr in the long-term climatic evolution in Central Asia.

The resulting orbital time scale also allows the correlation of climate changes at southern Tajikistan with other well-established climate records in the world, and the calculation of dust sedimentation rate (SR) for each of the loess–soil units (Fig. 7). The SR values (Fig. 7F) mostly vary between 0.05 and 0.3 m/kyr. In general, the eolian sedimentation rate of loess horizons is much higher than that of the overlying paleosols, indicating a dustier and drier environment during glacial periods compared with interglacial times. This is consistent with glacial–interglacial mass accumulation rate (MAR) variability of atmospheric dust over the Northwest Pacific Ocean, as recorded by deep-sea core V21-146 (Fig. 7E) [36]. Throughout the Pleistocene, there is a general upward increase in SR at Chashmanigar, implying that the deserts of Central Asia are developing toward a drier environment during the Quaternary. This trend is also generally coincident with the ODP 885/886 MAR record derived from the northwestern Pacific (Fig. 7E) [35,37].

Fig. 7 also shows the correlation of the grain size and color reflectance records at Chashmanigar (Fig. 7A,B) with the Lingtai grain size record in China (Fig. 7C) and the ODP 677 oxygen isotope record in the equatorial Pacific (Fig. 7D). The Lingtai loess section is located in the middle part of the Chinese Loess Plateau (Fig. 1a). It has a thickness of about 175 m and is composed of the S0–L33 loess–soil units with a basal age of about 2.6 Myr [24]. According to field observations and climatic proxy records, the Lingtai loess section can be regarded as representative of the Quaternary loess sediments in China. The grain

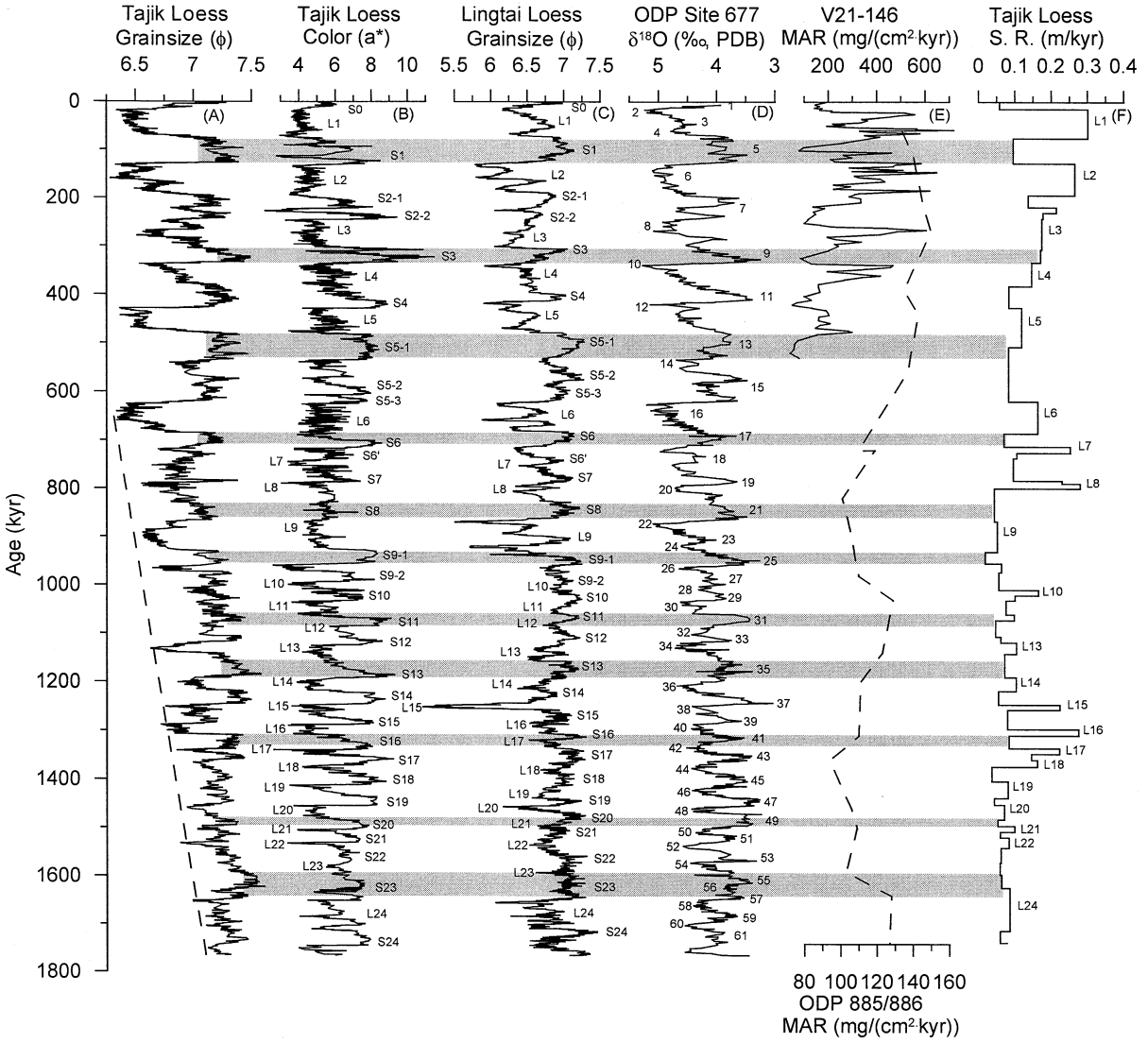

Fig. 7. Correlation of the Chashmanigar median grain size (A) and color reflectance (B) records with the Lingtai median grain size (C), ODP 677 $\delta^{18}O$ (D) [29], and V21-146 [36] and ODP 885/886 [37] eolian MAR (E) records. Averaged dust sedimentation rate, calculated using the CGS time scale, for each of the loess–soil units at Chashmanigar is shown (F). The loess–soil units in both the Chashmanigar and Lingtai loess records and the glacial–interglacial stages in the ODP 677 $\delta^{18}O$ record are all labeled.

size record at Lingtai has been published in [38]. In this study, we also tuned the Lingtai grain size record to variations in the orbital obliquity and precession of the Earth. The time scale of the ODP site 677 $\delta^{18}O$ time series [29] was generated by tuning the $\delta^{18}O$ record to the output of the model described in [39].

The similarity of the climatic records is manifested mainly in two aspects. Firstly, variations in the median grain size and color reflectance of the Chashmanigar loess can be correlated to the Lingtai median grain size and the ODP 677 oxygen isotope records almost cycle by cycle. This cycle-to-cycle correlation is more obvious between the Chashmanigar color reflectance and the oxygen isotope records in the early Pleistocene. Even

within some thick loess units (e.g. L2), the second-order climatic variations can be well correlated between the Chashmanigar and Lingtai grain size records. Secondly, climatic variability in the early Pleistocene is characterized by relatively high frequencies with reduced amplitudes for all the records. In the late Pleistocene, however, climatic frequencies become lower, with an obvious increase in amplitudes (Fig. 7). This event is accompanied by a shift of dominant climatic periodicity from 41 kyr to 100 kyr at about 1.0–0.8 Myr (Fig. 6).

Despite the similarities, discrepancies are also evident among the records. The most striking one lies in the fact that there is a consistent increase in the median grain size from 1.77 Myr to about 0.65 Myr for the Chashmanigar section, whereas this trend is absent in the Lingtai grain size and Chashmanigar color reflectance records. Although a slight trend of this kind can also be seen in the oxygen isotope record over this time interval, we believe that it is most likely a local event in southern Tajikistan because of the striking expression of the trend in the Chashmanigar grain size record. In the Lingtai record, there are clearly expressed second-order grain size cycles within the thick loess units such as L2, L5, L6, and L9 (Fig. 7C). These cycles represent the influence of orbital precessional cyclicity on the climate of northern China. However, these second-order cycles are not well documented in either the Chashmanigar loess or the deep-sea isotope record. Another disagreement between the Lingtai and Chashmanigar grain size records is concerned with the loess units of L9 and L15. It has long been recognized that loess units L9 and L15 are among the thickest and coarsest in the entire loess sequence in China [2]. They are interpreted to represent the coldest and driest periods in the Quaternary on the Loess Plateau. However, these two extreme climatic events are not recorded by the Chashmanigar loess and ODP 677 $\delta^{18}O$ records (Fig. 7).

6. Discussion and conclusions

In studies of the Central Asian loess, there is a debate regarding the paleoclimatic interpretation for the alternation of loess and soil horizons in Central Asian loess deposits. Some authors assumed that the loess horizons in Central Asia were deposited during glacial periods, whereas paleosols formed during interglacial periods. However, another school of authors considered that paleosol formation is associated with pluvial events during glacial periods, while loess deposition corresponds to interglacial times (see review [10]). Measurements of multiple climatic proxies in the present study show that all the paleosols at Chashmanigar are characterized by finer grain size distributions, higher magnetic susceptibilities, higher chromaticity a^* values, and lower dust sedimentation rates, compared to the loess horizons. Therefore paleosols can be interpreted as having formed under relatively humid, calm, warm climatic conditions with low atmospheric dust loadings. During formation of the loess horizons, the climate in Central Asia would be dry, windy and cold with comparatively high atmospheric dust loadings. The correlation of the Chashmanigar climatic records with the Chinese loess and deep-sea $\delta^{18}O$ records (Fig. 7) indicates that the paleosols in Central Asia correspond to interglacial periods, whereas the loess horizons correspond to glacial periods.

The above interpretation is actually similar to that for the loess–soil alternations in China. However, the wind system transporting the Central Asian loess is essentially different from that for the Chinese loess. As mentioned above, transport and sedimentation of the loess in southern Tajikistan is closely related to the regional westerly winds during summer seasons, whereas the Chinese loess is thought to be transported by the northwesterly winter monsoonal winds originated in the Siberian area [19]. In addition, the present climate in southern Tajikistan is characterized by hot, dry summers and cold, wet winters, which is in striking contrast with the hot, wet summer and cold, dry winter climate in the Loess Plateau. The similarity between the loess records of southern Tajikistan and the Loess Plateau therefore implies that climatic changes in both regions during the Pleistocene may be controlled by the same forcing factors on hemispheric or global scales.

Spectral analyses on long-term climatic records both from deep-sea sediments and Chinese loess have shown that at about 1.0–0.8 Myr, there occurred a major shift of dominant periodicities from 41 kyr variations to 100 kyr oscillations [9,28,40–42]. To date, the cause for the mid-Pleistocene climatic transition is still a puzzle in paleoclimatology [43,44]. Although variation in eccentricity of the Earth's orbit has a distinct 100 kyr periodicity, it makes less than a 0.1% direct contribution to insolation changes on the Earth [32]. Besides, the 100 kyr climatic rhythms during the early Pleistocene, if detected in any climatic record, do not show a clear phase relation with the theoretical eccentricity record. Therefore the mid-Pleistocene climate transition is most likely caused by changes in internal forcing factors within the climate system [43,44]. The well-documented mid-Pleistocene transition at Chashmanigar and the agreement between climatic records of Tajik loess and deep-sea sediments both strongly suggest that the alternation of loess–soil units in southern Tajikistan could be forced by variations in global ice volume, supporting an earlier suggestion [11].

The comparison of climatic records between the Lingtai and Chashmanigar loess sections (Fig. 7) suggests that atmospheric dust deposition over both regions may be also closely associated with changes in regional forcing factors. The coarsening of loess particles from 1.77 Myr to about 0.65 Myr at Chashmanigar (Fig. 7) implies a gradual enhancement of the regional wind intensity and/or expansion of the Central Asian deserts during glacial periods. Although this phenomenon can be explained partly by the increase in global ice volume over this interval, it may be largely a reflection of gradual changes in regional climate boundary conditions. It is unclear at present which regional forcing factors are responsible for this trend. Perhaps tectonic change of this region may be one of the most important candidates.

The occurrence of the prominent coarse, thick loess beds such as L9 and L15 in the Chinese loess record is also difficult to explain by global ice volume forcing, because of the absence of these events in both the ODP 677 $\delta^{18}O$ and Chashmanigar loess records (Fig. 7). In the Chinese loess, paleosols are separated by thick loess horizons above L9, whereas they are closely spaced below it except for some thick loess beds. These thick loess beds are numbered L9, L15, L24, L27, L32, and L33 and are used as stratigraphic markers in field work [5]. The grain size distributions of L9, L15, and L33 are among the coarsest in the entire loess sequence, while L24, L27, and L32 are relatively coarser than other loess horizons below L9 [9,38]. Some authors speculated that the deposition of the coarse loess beds might be linked to tectonic uplift of mountains in Asia [3,45]. Mountain uplift implies a profound change in boundary conditions for the regional climate system, the effect of which should be retained on subsequent loess deposition. However, this expected effect does not occur in loess grain size records, thus challenging the tectonic explanation. Interestingly, the excursions of L9, L15, L24, L27, and the L32–L33 couplet occurred roughly at every 0.4 Myr, and the timing for most of the excursions is approximately consistent with the lowest values of the long wavelength cycles (the 0.413 Myr period) in the Earth's eccentricity record (not shown). This suggests that the regional climate system controlling atmospheric dust deposition in China may be more sensitive to the direct forcing of variations in the Earth's orbit than those affecting the loess sedimentation in Central Asia. The clear precessional 20 kyr cycles registered in grain size changes of L2, L5, L6, and L9, which are absent in both the Chashmanigar loess and ODP 677 $\delta^{18}O$ records (Fig. 7), further support this contention.

Acknowledgements

We thank Drs. David Rea, Andre Berger, David Heslop and an anonym for critical comments on an early version of this manuscript. This study is supported by the NNSF of China (49894170, 40024202) and CAS (KZCX2-108).[*RV*]

References

[1] F. Heller, T.S. Liu, Magnetostratigraphic dating of loess deposits in China, Nature 300 (1982) 431–433.

[2] T.S. Liu, Loess and the Environment, China Ocean Press, Beijing, 1985.
[3] G. Kukla, Loess stratigraphy in Central China, Quat. Sci. Rev. 6 (1987) 191–219.
[4] G. Kukla, Z.S. An, Loess stratigraphy in Central China, Palaeogeogr. Palaeoclimatol. Palaeoecol. 72 (1989) 203–225.
[5] N.W. Rutter, Z.L. Ding, M.E. Evans, T.S. Liu, Baoji-type pedostratigraphic section, Loess Plateau, north-Central China, Quat. Sci. Rev. 10 (1991) 1–22.
[6] S.C. Porter, Z.S. An, Correlation between climate events in the North Atlantic and China during the last glaciation, Nature 375 (1995) 305–308.
[7] E. Derbyshire, R.A. Kemp, X.M. Meng, Climate change, loess and palaeosols: proxy measures and resolution in North China, J. Geol. Soc. London 154 (1997) 793–805.
[8] A.A. Lazarenko, The Loess of Central Asia, in: Late Quaternary Environments of the Soviet Union, Lougruan, London, 1984, pp. 125–131.
[9] Z.L. Ding, Z.W. Yu, N.W. Rutter, T.S. Liu, Towards an orbital time scale for Chinese loess deposits, Quat. Sci. Rev. 13 (1994) 39–70.
[10] A.E. Dodonov, L.L. Baigusina, Loess stratigraphy of Central Asia: palaeoclimatic and palaeoenvironmental aspects, Quat. Sci. Rev. 14 (1995) 707–720.
[11] N.J. Shackleton, Z. An, A.E. Dodonov, J. Gavin, G. Kukla, V.A. Ranov, L.P. Zhou, Accumulation rate of loess in Tadjikistan and China: relationship with global ice volume cycles, Quat. Proc. 4 (1995) 1–6.
[12] T.S. Liu, Z.L. Ding, Chinese loess and the paleomonsoon, Annu. Rev. Earth Planet. Sci. 26 (1998) 111–145.
[13] Z.S. An, G. Kukla, S.C. Porter, J.L. Xiao, Magnetic susceptibility evidence of monsoon variation on the Loess Plateau of Central China during the last 130,000 years, Quat. Res. 36 (1991) 29–36.
[14] Z.L. Ding, T.S. Liu, N.W. Rutter, Z.W. Yu, Z.T. Guo, R.X. Zhu, Ice-volume forcing of the east Asia winter monsoon variations in the past 800,000 years, Quat. Res. 44 (1995) 149–159.
[15] A.E. Dodonov, Loess of Central Asia, GeoJournal 24 (1991) 185–194.
[16] A.E. Dodonov, N.J. Shackleton, L.P. Zhou, S.P. Lomov, A.F. Finaev, Quaternary loess-paleosol stratigraphy of Central Asia: geochronology, correlation and evolution of paleoenvironments, Stratigr. Geol. Correl. 7 (1999) 581–593.
[17] A. Finaev, Processes of transportation and sedimentation of dust aerosol, in: Global Analysis, Interpretation and Modeling, First Science Conference 25–29 September 1995, Garmisch-Partenkirchen, IGBP Secretariat of Germany in Berlin, 1995, p. 22.
[18] Z.L. Ding, J.Z. Ren, S.L. Yang, T.S. Liu, Climate instability during the penultimate glaciation: evidence from two high-resolution loess records, China, J. Geophys. Res. 104 (1999) 20123–20132.
[19] Z.S. An, G. Kukla, S.C. Porter, J.L. Xiao, Late Quaternary dust flow on the Chinese Loess Plateau, Catena 18 (1991) 125–132.
[20] Z.L. Ding, J.M. Sun, N.W. Rutter, D. Rokosh, T.S. Liu, Changes in sand content of loess deposits along a north-south transect of the Chinese Loess Plateau and the implications for desert variations, Quat. Res. 52 (1999) 56–62.
[21] X.M. Liu, T. Rolph, J. Bloemendal, J. Shaw, T.S. Liu, Quantitative estimates of palaeoprecipitation at Xifeng area, in the Loess Plateau of China, Palaeogeogr. Palaeoclimatol. Palaeoecol. 113 (1995) 243–248.
[22] F. Heller, M.E. Evans, Loess magnetism, Rev. Geophys. 33 (1995) 211–240.
[23] N.W. Rutter, Z.L. Ding, M.E. Evans, Y.C. Wang, Magnetostratigraphy of the Baoji loess-paleosol section in the north-Central China Loess Plateau, Quat. Int. 7/8 (1990) 97–102.
[24] Z.L. Ding, J.M. Sun, S.L. Yang, T.S. Liu, Preliminary magnetostratigraphy of a thick eolian red clay-loess sequence at Lingtai, the Chinese Loess Plateau, Geophys. Res. Lett. 25 (1998) 1225–1228.
[25] M.M. Milankovitch, Kyrnon der Erdestrahlung, Koninglich Serbische Akyrdemie, Beograd, 1941. (English translation: Canon of Insolation and the Ice Age Problem, by Israel Program for Scientific Translation and published for the US Department of Commerce and the National Science Foundation.)
[26] J.D. Hays, J. Imbrie, N.J. Shackleton, Variations in the Earth's orbit: pacemaker of the ice ages, Science 194 (1976) 1121–1132.
[27] J. Imbrie, J.D. Hays, D.G. Martinson, A. McIntyre, A.C. Mix, J.J. Morley, N.G. Pisias, W.L. Prell, N.J. Shackleton, The orbital theory of Pleistocene climate: support from a revised chronology of the marine $\delta^{18}O$ record, in: A. Berger, J. Imbrie, J. Hays, G. Kukla, B. Saltzman (Eds.), Milankovitch and Climate: Understanding the Response to Astronomical Forcing, Part I, D. Reidel, Dordrecht, 1984, pp. 269–305.
[28] W.F. Ruddiman, M.E. Raymo, D.G. Martinson, S.C. Clemens, J. Backman, Pleistocene evolution: northern Hemisphere ice sheets and North Atlantic Ocean, Paleoceanography 4 (1989) 353–412.
[29] N.J. Shackleton, A. Berger, W.R. Peltier, An alternative astronomical calibration of the lower Pleistocene timescale based on ODP site 677, Transaction of Royal Society of Edinburgh, Earth Sci. 81 (1990) 251–261.
[30] J. Chen, J.W. Farrell, D.W. Murray, W.L. Prell, Timescale and paleoceanographic implications of a 3.6 m.y. oxygen isotope record from the northeast Indian Ocean (Ocean Drilling Program site 758), Paleoceanography 10 (1995) 21–47.
[31] D. Heslop, C.G. Langereis, M.J. Dekkers, A new astronomical timescale for the loess deposits of Northern China, Earth Planet. Sci. Lett. 184 (2000) 125–139.
[32] A. Berger, M.F. Loutre, Insolation values for the climate of the last 10 million years, Quat. Sci. Rev. 10 (1991) 297–317.
[33] L.P. Zhou, N.J. Shackleton, Misleading positions of geomagnetic reversal boundaries in Eurasian loess and impli-

cations for correlation between continental and marine sedimentary sequences, Earth Planet. Sci. Lett. 168 (1999) 117–130.
[34] Z.W. Yu, Z.L. Ding, An automatic orbital tuning method for paleoclimate records, Geophys. Res. Lett. 25 (1998) 4525–4528.
[35] D.K. Rea, The paleoclimatic record provided by eolian deposition in the deep sea: the geologic history of wind, Rev. Geophys. 32 (1994) 159–195.
[36] S.A. Hovan, D.K. Rea, N.G. Pisias, Late Pleistocene continental climate and oceanic variability recorded in northwest Pacific sediments, Paleoceanography 6 (1991) 349–370.
[37] D.K. Rea, H. Snoeckx, L.H. Joseph, Late Cenozoic eolian deposition in the North Pacific: Asian drying, Tibet uplift, and cooling of the Northern Hemisphere, Paleoceanography 13 (1998) 215–224.
[38] Z.L. Ding, S.F. Xiong, J.M. Sun, S.L. Yang, Z.Y. Gu, T.S. Liu, Pedostratigraphy and paleomagnetism of a ~7.0 Ma eolian loess-red clay sequence at Lingtai, Loess Plateau, north-Central China and the implications for paleomonsoon evolution, Palaeogeogr. Palaeoclimatol. Palaeoecol. 152 (1999) 49–66.
[39] J. Imbrie, J.Z. Imbrie, Modeling the climatic response to orbital variations, Science 207 (1980) 943–953.
[40] N.G. Pisias, T.C. Moore, The evolution of Pleistocene climate: a time series approach, Earth Planet. Sci. Lett. 52 (1981) 450–458.
[41] W.L. Prell, Oxygen and carbon isotopic stratigraphy for the Quaternary of hole 502B: evidence for two modes of isotopic variability, Initial Rep. Deep Sea Drill. Proj. 68 (1982) 455–464.
[42] W.F. Ruddiman, M. Raymo, A. McIntyre, Matuyama 41,000 years cycles: North Atlantic Ocean and northern Hemisphere ice sheets, Earth Planet. Sci. Lett. 80 (1986) 117–129.
[43] M.E. Raymo, D.W. Oppo, W. Curry, The mid-Pleistocene climate transition: a deep sea carbon isotopic perspective, Paleoceanography 12 (1997) 546–559.
[44] P.U. Clark, R.B. Alley, D. Pollard, Northern Hemisphere ice-sheet influences on global climate change, Science 286 (1999) 1104–1111.
[45] J.M. Sun, T.S. Liu, Stratigraphic evidence for the uplift of the Tibetan Plateau between ~1.1 and ~0.9 myr ago, Quat. Res. 54 (2000) 309–320.